

# Synthesis and structural characterisation of $[\text{Cu}_2[(\text{PDC})_2(\text{bpa})(\text{H}_2\text{O})_2] \cdot n\text{H}_2\text{O} \cdot m\text{DMF}]$ ( $n=3$ and $m=1$ for **1**, $n=7$ and $m=0$ for **2**, PDC=2,5-pyridinedicarboxylate and bpa= 1,2-di(4-pyridil)ethane))

Begoña Bazán,<sup>a,b</sup> Gotzone Barandika,<sup>c</sup> Francisco Llano-Tomé,<sup>a</sup> Miren-Karmele Urtiaga<sup>a</sup> and María-Isabel Arriortua<sup>a,b</sup>

<sup>a</sup>Departamento de Mineralogía y Petrología, Facultad de Ciencia y Tecnología, Universidad del País Vasco (UPV/EHU), Apdo 644, 48080 Bilbao, Spain.

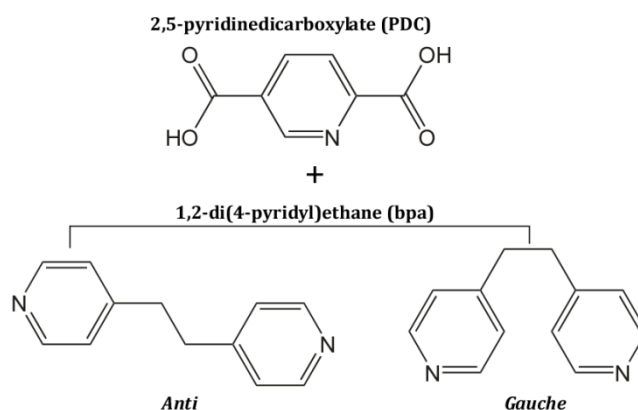
<sup>b</sup>BCMaterials Parque Tecnológico de Zamudio, Ibaizabal Bidea, Edificio 500-Planta 1, 48160, Derio, Spain.

<sup>c</sup>Departamento de Química Inorgánica, Facultad de Ciencia y Tecnología, Universidad del País Vasco (UPV/EHU), Apdo 644, 48080 Bilbao, Spain.

## 1. Experimental Section

### 1.1. Materials and general methods

All solvents and chemicals were used as received from reliable commercial sources. The reactants, 2,5-pyridinedicarboxylic acid ( $\text{H}_2\text{PDC}$ ), 1,2-di(4-pyridyl)ethane, copper (II) nitrate hydrated 99%, triethylamine ( $\text{Et}_3\text{N}$ ) and the solvent N,N-dimethylformamide (DMF) 99.8%, were purchased from Sigma-Aldrich Co. The nitric acid 65% ( $\text{HNO}_3$ ) and ethanol (EtOH) 96% were purchased from Panreac.



**Scheme 1** Lewis structure for PDC and bpa ligands

The thermogravimetric analysis (TGA) was performed under air atmosphere on a SDT 2960 Simultaneous DSC-TGA TA Instrument. The IR spectra were obtained with a Jasco FT/IR-6100 spectrophotometer in the  $400\text{--}4000\text{ cm}^{-1}$  range with pressed KBr pellets. C, H and N elemental analyses were measured using a Euro EA 3000 Elemental analyzer.

### 1.2. Synthesis of $[\text{Cu}_2[(\text{PDC})_2(\text{bpa})(\text{H}_2\text{O})_2]\cdot 3\text{H}_2\text{O}\cdot \text{DMF}]$ (1)

$\text{H}_2\text{PDC}$  (40.4 mg, 0.25 mmol),  $\text{bpa}$  (46.3 mg, 0.25 mmol) and  $\text{Cu}(\text{NO}_3)_2\cdot 6\text{H}_2\text{O}$  (93.3 mg, 0.5 mmol) were dissolved in a solvent mixture of  $\text{DMF}/\text{H}_2\text{O}$  (10/10 mL) after stirring for 1h at RT. The pH value was adjusted to 4.5 using  $\text{Et}_3\text{N}$  and  $\text{HNO}_3$  (0,5 M). The resulting solution was sealed in a teflon-lined autoclave for microwaves (XP1500), heating at  $140^\circ\text{C}$  during 45 min in order to improve the solubility of the reagents. Then, the solution was filtered and dropped in a glass crystallizing dish. After twelve hours, blue prismatic crystals were obtained. The sample was washed and dried with ethanol, collecting a crystal for X-ray diffraction experiment. The density was measured by the flotation method in a mixture of bromoform/choloroform being  $1.68(5) \text{ g}\cdot\text{cm}^{-3}$  (Found: C, 43.1(2); H, 3.95(2); N, 8.43(3). Calc. for  $\text{C}_{29}\text{H}_{35}\text{Cu}_2\text{N}_5\text{O}_{14}$ : C, 43.24; H, 4.35; N, 8.70. IR:  $\nu_{\text{max}}/\text{cm}^{-1}$  3424 (OH), 1656 and 1622 (aroC-C), 1281 (C-N), 1560 (asCOO), 1425, 1389 and 1352 (sCOO), 835, 768 and 693 (C-H) and 549-532 (Cu-N) (figure 1).

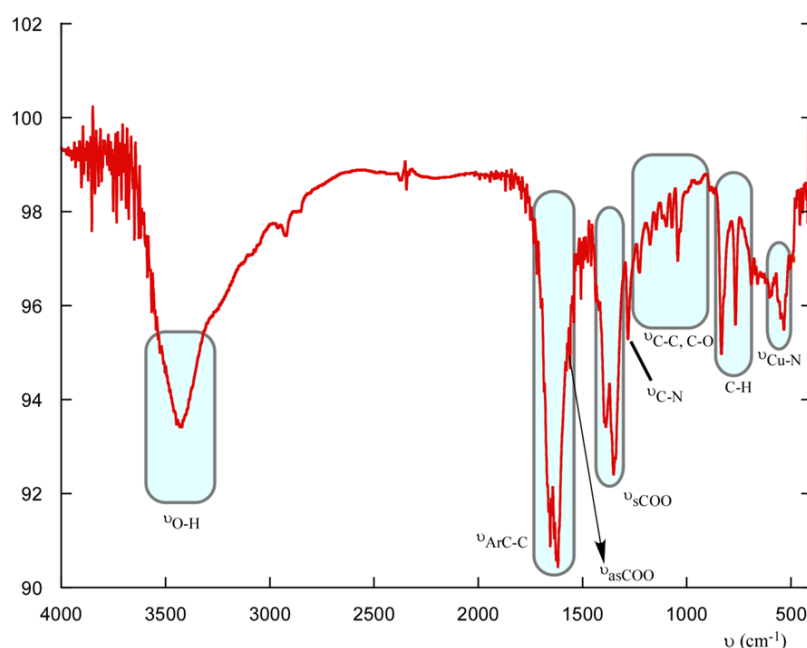


**Figure 1.** IR spectra for compound **1** ( $\text{C}_{29}\text{H}_{35}\text{N}_5\text{O}_{14}\text{Cu}_2$ ). The following bands ( $\text{cm}^{-1}$ ) are marked: 3424 (OH), 1656 and 1622 (aroC-C), 1281 (C-N), 1560 (asCOO), 1425, 1389 and 1352 (sCOO), 835, 768 and 693 (C-H) and 549-532 (Cu-N).

### 1.3. Synthesis of $[\text{Cu}_2(\text{PDC})_2(\text{bpa})(\text{H}_2\text{O})_2]\cdot 7\text{H}_2\text{O}$ (2)

$\text{H}_2\text{PDC}$  (93.3 mg, 0.5 mmol),  $\text{bpa}$  (81.1 mg, 0.5 mmol) and  $\text{Cu}(\text{NO}_3)_2\cdot 2.5\text{H}_2\text{O}$  were dissolved in a solvent mixture of  $\text{H}_2\text{O}/\text{EtOH}$  (20/10 mL) after stirring for 1h at  $60^\circ\text{C}$ . The resulting solution was filtered and dropped in a glass crystallizing dish. After several days, blue prismatic crystals were obtained. The sample was washed with ethanol, collecting a crystal for X-ray diffraction experiment. The density was measured by the flotation method in a mixture of bromoform/chloroform being  $1.58(5) \text{ g}\cdot\text{cm}^{-3}$  (Found: C, 39.1(2); H, 4.24(2); N, 6.75(3). Calc. for  $\text{C}_{26}\text{H}_{36}\text{Cu}_2\text{N}_4\text{O}_{17}$ : C, 38.82; H, 4.48; N, 6.96. IR:  $\nu_{\text{max}}/\text{cm}^{-1}$  3415 (OH), 1652 and 1617 (aroC-C), 1284 (C-N), 1568 (asCOO), 1428, 1398 and 1352 (sCOO), 837, 768 and 690 (C-H) and 552-538 (Cu-N) (figure 2).

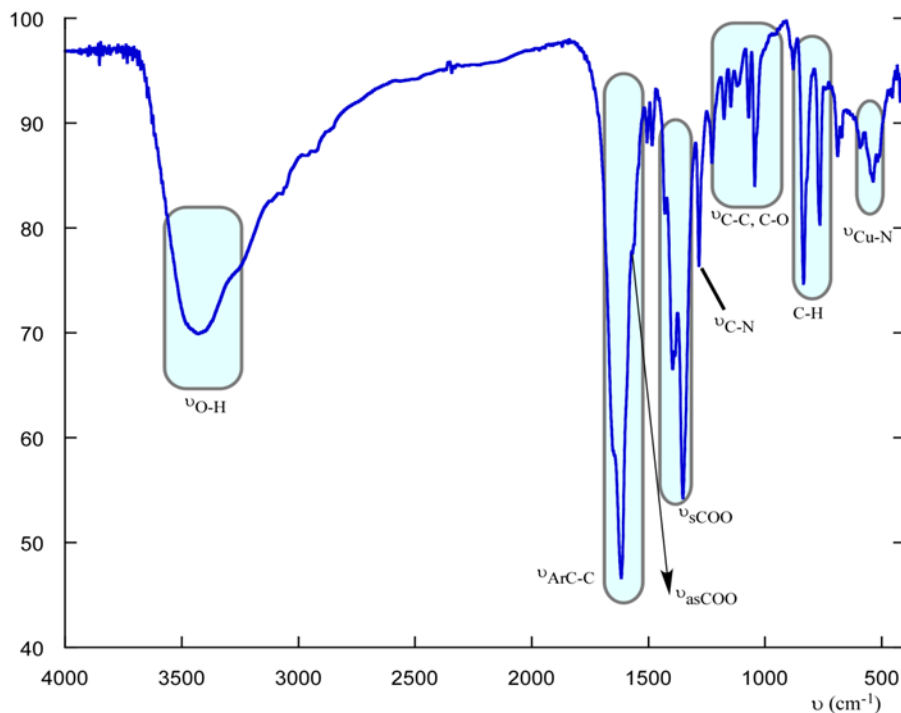


**Figure 2.** IR spectra for compound **2** ( $C_{26}H_{36}N_4O_{17}Cu_2$ ). The following bands ( $cm^{-1}$ ) are marked: 3415 (OH), 1652 and 1617 (aroC-C), 1284 (C-N), 1568 (asCOO), 1428, 1398 and 1352 (sCOO), 837, 768 and 690 (C-H) and 552-538 (Cu-N).

#### 1.4. Single-crystal X-ray diffraction

Prismatic single-crystals of compounds **1** and **2** with dimensions given in table 1 were selected under polarizing microscope and mounted on MicroMounts. Single-crystal data were collected at 100 K on an Agilent Technologies Supernova single source diffractometer with Cu-K $\alpha$  radiation (1.54184 Å) for compound **1** and Mo-K $\alpha$  (0.71073 Å) radiation for compound **2**. Details of crystal data and some features of the structures refinements are reported in table 1, and selected bond length and angles are listed in tables 2 and 3.

Lattice constants were obtained by using a standard program belonging to the diffractometer software, confirming at the same time the good quality of the single-crystals. The Lorentz polarization and absorption corrections were made with the diffractometer software, taking into account the size and shape of the crystals [1]. The structures were solved by direct methods using SIR92 program [2], with the monoclinic *Pn* space group for compound **1**, and the *C2/c* for compound **2**, which allowed us to obtain the positions of the copper atoms, as well as the oxygen and nitrogen atoms and some of the carbon atoms of both PDC and bpa ligands of compounds **1** and **2**. The refinement of the crystal structures was performed by full-matrix least-squares based on  $F^2$ , using the SHELXL-97 program [3], obtaining the remaining carbon atoms and allowing the allocation of the hydrogen atoms. Anisotropic thermal parameters were used for all non-hydrogen atoms (figures 3 and 4). The hydrogen atoms belonging to the organic molecules were fixed geometrically and allowed the ride on their parent carbon atoms (C-H 0.93 Å), and were refined with common isotropic displacements. The position of the hydrogen atoms bonded to the coordinating water molecules of

compounds **1** and **2**, as well as the hydrogen atoms bonded to the crystallization water molecules of compound **1**, were fixed using DFIX and DANG instructions in the refinement to adjust the O-H distance to 0.82 Å and the H-O-H angle to 112°, respectively. In compound **2**, there is one crystallization molecule of water disordered in two parts, and another one is situated in a special position, being its occupancy of 0.5. The hydrogen atoms of these water molecules were not considered due to the lack of density in the residual density map. Attempts to solve the structure for **1** in  $P2_1/n$  were fruitless.

**Table 1** Details of the crystal data, structural resolution and refinement procedure for **1** and **2**

Compounds	<b>1</b>	<b>2</b>
Formula	C <sub>29</sub> H <sub>35</sub> N <sub>5</sub> O <sub>14</sub> Cu <sub>2</sub>	C <sub>26</sub> H <sub>36</sub> N <sub>4</sub> O <sub>17</sub> Cu <sub>2</sub>
FW, g·mol <sup>-1</sup>	804.70	803.67
Crystal system	Monoclinic	Monoclinic
S.G. (n°)	<i>Pn</i> , (7)	<i>C2/c</i> , (15)
<i>a</i> , Å	11.4795(10)	18.8827(5)
<i>b</i> , Å	8.8862(10)	9.8114(2)
<i>c</i> , Å	15.9648 (10)	19.5013(4)
$\beta$ , °	93.7080(10)	108.692
<i>V</i> , Å <sup>3</sup>	1625.15(3)	3422.36(13)
<i>Z</i> , <i>F</i> (000)	2, 828	4, 1600
$\rho_{obs}$ , $\rho_{cal}$ , g·cm <sup>-3</sup>	1.68(5), 1.64	1.58(5), 1.56
$\mu$ , mm <sup>-1</sup>	2.30	1.321
Crystal size, mm	0.103 x 0.077 x 0.067	0.108 x 0.162 x 0.12
Radiation, $\lambda$ , Å	1.54184	0.71073
Temperature, K	100.0(10)	100.0(10)
Reflections collected, unique	27613, 6660 ( <i>R</i> <sub>int</sub> = 0.024)	12908, 3878 ( <i>R</i> <sub>int</sub> = 0.027)
Limiting indices	-14 <= <i>h</i> <= 14 -11 <= <i>k</i> <= 11 -20 <= <i>l</i> <= 20	-23 <= <i>h</i> <= 24 -13 <= <i>k</i> <= 12 -21 <= <i>l</i> <= 25
Final <i>R</i> indices [ <i>I</i> > 2 $\sigma$ ( <i>I</i> )] <sup>a</sup>	<i>R</i> <sub>1</sub> = 0.024, w <i>R</i> <sub>2</sub> = 0.067	<i>R</i> <sub>1</sub> = 0.040, w <i>R</i> <sub>2</sub> = 0.101
<i>R</i> indices (all data) <sup>a</sup>	<i>R</i> <sub>1</sub> = 0.024, w <i>R</i> <sub>2</sub> = 0.068	<i>R</i> <sub>1</sub> = 0.047, w <i>R</i> <sub>2</sub> = 0.105
Goodness of fit on <i>F</i> <sup>2</sup>	1.011	1.098
Parameters / restraints	494 / 8	238 / 3
L. Diff. peak and hole (e Å <sup>-3</sup> )	0.625, -0.338	1.451, -0.986

**Table 2.** Selected bond angles (°) and distances (Å) for compound **1** (distances in bold).

<b>Cu1</b>	<b>O1</b>	<b>O7</b>	<b>O2W</b>	<b>N2</b>	<b>N3</b>
<b>N3</b>	91.50(8)	91.06(8)	99.69(7)	169.92(8)	<b>2.0133(19)</b>
<b>N2</b>	95.68(7)	81.66(8)	87.20(7)	<b>2.026(2)</b>	
<b>O2W</b>	91.70(7)	88.88(7)	<b>2.2488(18)</b>		
<b>O7</b>	177.25(7)	<b>1.9520(17)</b>			
<b>O1</b>	<b>1.9445(16)</b>				
<b>Cu2</b>	<b>O3<sup>i</sup></b>	<b>O5</b>	<b>O1W</b>	<b>N1<sup>i</sup></b>	<b>N4</b>
<b>N4</b>	91.92(7)	92.09(7)	99.67(7)	168.77(8)	<b>2.0366(19)</b>
<b>N1<sup>i</sup></b>	81.57(7)	94.08(7)	89.25(7)	<b>2.024(2)</b>	
<b>O1W</b>	87.70(7)	94.06(7)	<b>2.2197(16)</b>		
<b>O5</b>	175.29(7)	<b>1.9340(16)</b>			
<b>O3<sup>i</sup></b>	<b>1.9693(16)</b>				

i) *x*, 1+*y*, *z*

**Table 3.** Selected bond angles ( $^{\circ}$ ) and distances ( $\text{\AA}$ ) for compound **2** (distances in bold).

Cu1	O1	O3	O5W	N1	N2
N2	81.68(8)	91.62(8)	93.54(8)	172.31(9)	<b>1.999(2)</b>
N1	92.43(8)	92.82(8)	91.78(9)	<b>1.992(2)</b>	
O5W	94.64(8)	101.00(8)	<b>2.259(2)</b>		
O3	163.32(8)	<b>1.9898(17)</b>			
O1	<b>1.9737(18)</b>				

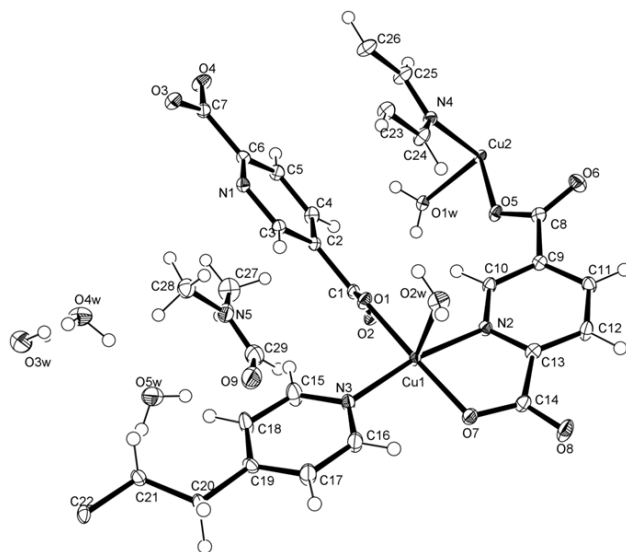


**Figure 3** Thermal ellipsoid plot (50% of probability) for compound **1**.

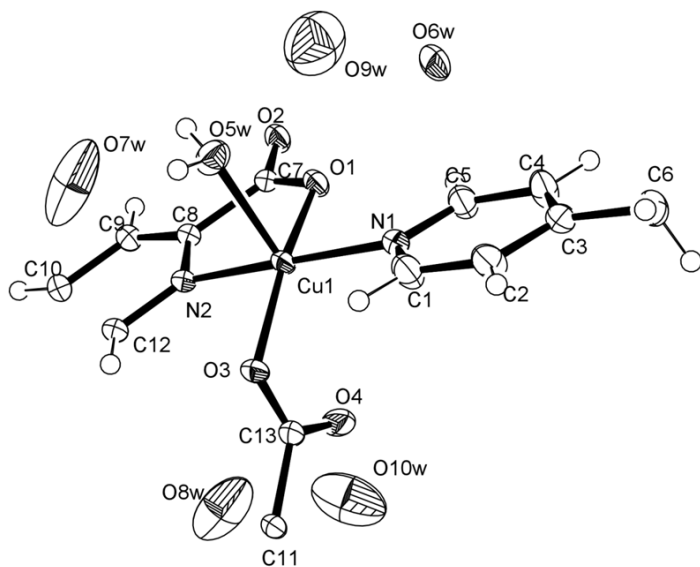


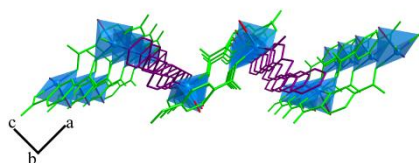
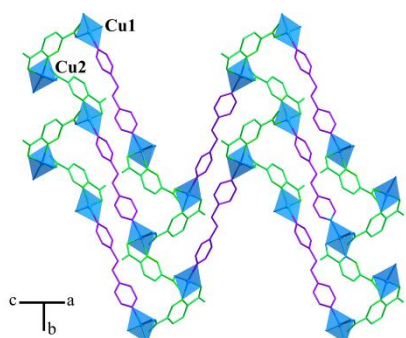
**Figure 4.** Thermal ellipsoid plot (50% of probability) for compound **2**.

## 2. Structural characterisation

### 2.1. Crystal structures

Crystal structures for compounds  $[\text{Cu}_2(\text{PDC})_2(\text{bpa})(\text{H}_2\text{O})_2]\cdot 3\text{H}_2\text{O}\cdot \text{DMF}$  (**1**), and  $[\text{Cu}_2(\text{PDC})_2(\text{bpa})(\text{H}_2\text{O})_2]\cdot 7\text{H}_2\text{O}$  (**2**) are quite similar, so they will be described together. In fact, both compounds consist of 2D arrays of the 3-c herringbone-type (figure 5). We have recently reported on similar arrays for Cu-PDC-bpe systems (bpe=(1,2-di(4-pyridyl)ethene) [4] For both compounds, Cu atoms have square pyramidal coordination environment, being coordinated to two oxygen atoms and a nitrogen atom (from two different PDC ligands) and to a nitrogen atom belonging to a bpa ligand in the equatorial plane and to a water molecule in the apical position. (figure 3 and 4).

Compound 1



Compound 2

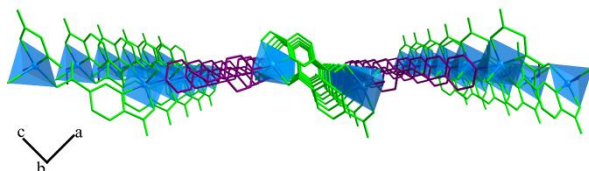
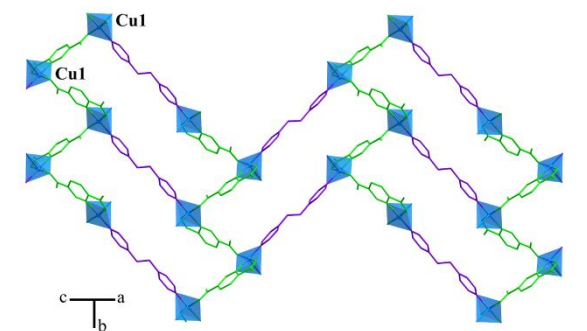


**Figure 5** Herringbone arrays of the 3-c type for (top) compound **1** and (bottom) compound **2**. Colour codes:  $\text{Cu}^{\text{II}}$  polyhedra in blue, PDC ligands in green and bpa in purple (all hydrogen atoms are omitted for clarity)

As observed in figure 5, herringbone arrays exhibit different angles and distances which will be discussed below. These differences are based on the distinct torsion angles for bpa in compounds **1** ( $10.15^\circ$ ) and **2** ( $5.55^\circ$ ). Both angles correspond to the

*anti* conformation. On the other hand, PDC ligands linking Cu1 and Cu2 in **1** are rotated in comparison to the ones linking equivalent Cu1 in **2** (figure 6).

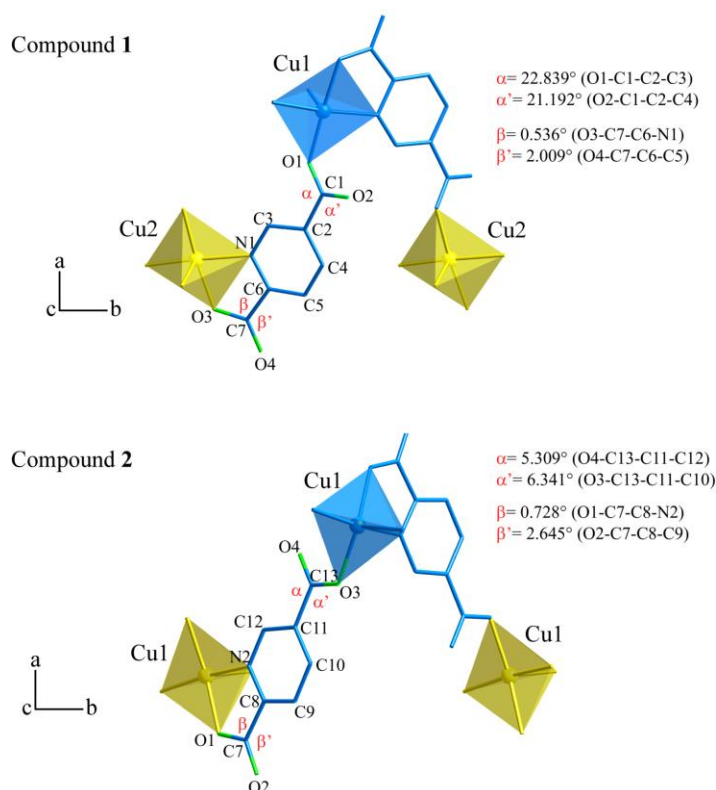


**Figure 6.** Torsion angles for the carboxylic groups of the PDC ligand.

These herringbone layers are interconnected via hydrogen bonds (tables 4 and 5) through the crystallization molecules (1 DMF and 3 H<sub>2</sub>O molecules per 2 Cu atoms in compound **1**, and 7 H<sub>2</sub>O molecules per 2 Cu atoms in compound **2**, giving rise to a 3D supramolecular framework (figure 7). with channels along the [010] direction.

**Table 4.** Interlayer Hydrogen bonds for compound **1**.

O-H	A(O)	O-H(Å)	H...A (Å)	O...A (Å)	O-H...A (°)
O(3W)-H(3AW)	O(4W)	0.95(3)	1.89(3)	2.824(2)	169(2)
O(3W)-H(3BW)	O(6) -1/2+x, 2-y, -1/2+z	0.83(4)	1.81(4)	2.630(4)	166(5)
O(1W)-H(1AW)	O(8) -1+x, y, z	0.819(18)	1.883(18)	2.700(2)	175(2)
O(1W)-H(1BW)	O(4W) x, 1+y, z	0.81(2)	1.94(2)	2.740(2)	168(2)
O(4W)-H(4BW)	O(5W)	0.88(3)	1.81(3)	2.659(3)	162(3)
O(4W)-H(4AW)	O(2) x, -1+y, z	0.85(3)	1.91(3)	2.752(2)	172(2)
O(5W)-H(5AW)	O(9)	0.843(11)	1.923(11)	2.746(2)	165(2)
O(2W)-H(2AW)	O(3W)1/2+x,1- y,1/2+z	0.82(3)	1.97(3)	2.761(3)	162(3)
O(2W)-H(2BW)	O(4) 1+x, y, z	0.73(3)	2.12(3)	2.834(2)	166(3)
O(5W)-H(5BW)	O(4) 1/2+x, 1-y, -1/2+z	0.837(19)	1.95(2)	2.783(3)	173(3)
C(5)-H(5)	O(8) -1+x, y, z	0.95(3)	2.53(2)	3.258(3)	133(2)
C(10)-H(10)	O(2)	0.95(3)	2.47(4)	3.172(3)	131(2)
C(10)-H(10)	O(5)	0.95(3)	2.39(3)	2.715(3)	100(3)
C(15)-H(15)	O(1)	0.95(3)	2.40(3)	2.932(3)	115(2)
C(16)-H(16)	O(7)	0.95(3)	2.39(4)	2.917(3)	115(2)
C(18)-H(18)	O(5W)	0.95(3)	2.51(3)	3.362(3)	150(3)
C(24)-H(24)	O(5)	0.95(3)	2.34(4)	2.923(3)	119(2)
C(25)-H(25)	O(3) x, 1+y, z	0.95(3)	2.33(4)	2.922(3)	119(2)

<b>C(25)-H(25)</b>	O(9) -1/2+x, 2-y, 1/2+z	0.95(3)	2.57(3)	3.226(3)	126(3)
<b>C(28)-H(28)</b>	O(5W)	0.98(3)	2.54(3)	3.298(3)	134(3)
<b>C(15)-H(15)</b>	O(9)	0.95(2)	2.712(2)	3.426(3)	132(2)
<b>C(26)-H(26)</b>	O(9) x-1/2, -y+2, z+1/2	0.95(2)	2.709(2)	3.285(3)	120(2)

**Table 5.** Interlayer Hydrogen bonds for compound **2**.

O-H	A(O)	O-H(Å)	H...A (Å)	O...A (Å)	O-H...A (°)
<b>O(5w)-H(5BW)</b>	O(2)1/2-x,3/x-y, z	0.82(4)	1.94(5)	2.757(3)	175(6)
<b>O(5w)-H(5AW)</b>	O(7w)	0.82(4)	1.95(4)	2.752(3)	167(6)
<b>C(1)-H(1)</b>	O(3)	0.95(4)	2.48(4)	2.982(4)	113(3)
<b>C(2)-H(2)</b>	O(8W) x+1/2, y-1/2, z	0.95(3)	2.766(4)	3.595(4)	146(2)
<b>C(4)-H(4)</b>	O(10W)-x+1/2,-y+1/2,-z	0.95(3)	2.429(1)	3.085(2)	126(2)
<b>C(5)-H(5)</b>	O(1)	0.95(4)	2.36(5)	2.930(4)	118(3)
<b>C(6)-H(6A)</b>	O(8W) x+1/2, y-1/2, z	0.99(3)	2.673(3)	3.438(4)	134(2)
<b>C(6)-H(6A)</b>	O(10W) x+1/2, y-1/2, z	0.99(3)	2.976(2)	3.563(2)	119(2)
<b>C(9)-H(9)</b>	O(9W) -x+1/2,-y+1/2+1,-z	0.95(2)	2.895(6)	3.799(6)	159(2)
<b>C(10)-H(10)</b>	O(9W)-1/2+x, 1/2+y, z	0.95(3)	2.56(4)	3.388(7)	146(4)
<b>C(12)-H(12)</b>	O(3)	0.95(3)	2.56(4)	3.049(4)	112(4)
<b>C(12)-H(12)</b>	O(10W)	0.95(2)	2.647(1)	3.382(9)	134(2)
<b>C(12)-H(12)</b>	O(4)1/2-X,1/2+y, 1/2-z	0.95(4)	2.47(4)	2.787(3)	100(4)

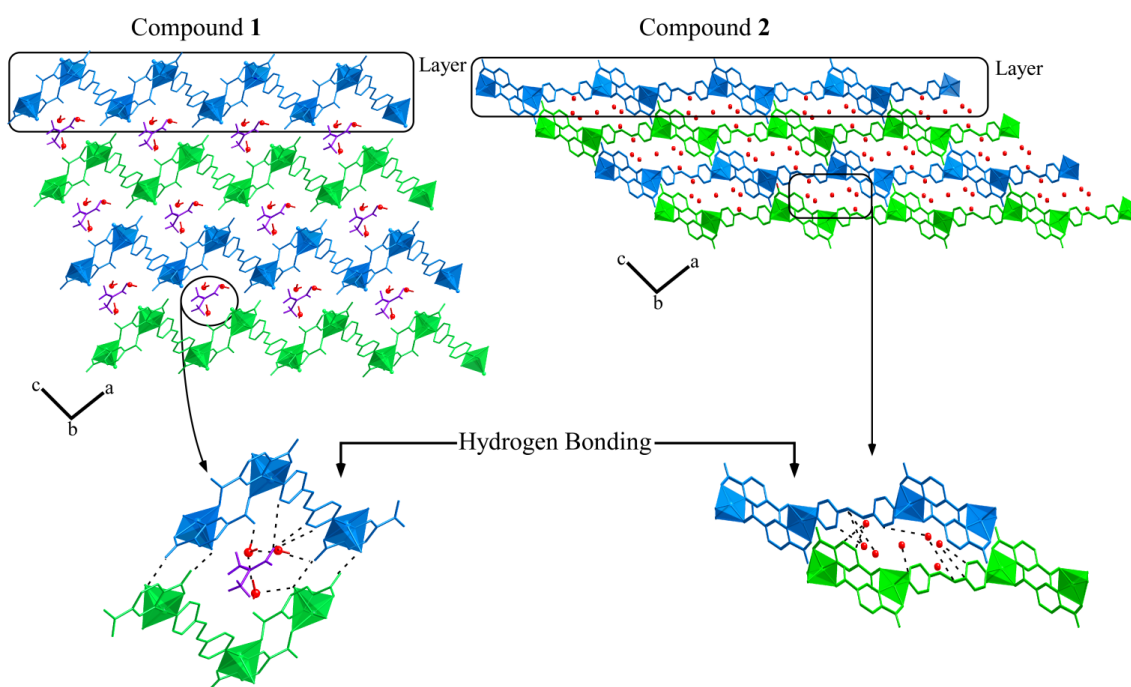


**Figure 7** 3D supramolecular framework for (left) compound **1** and (right) compound **2**. Crystallization molecules of water are shown in red, and DMF molecules in violet. Zoomed images at the bottom show the hydrogen bonds as dashed lines (all hydrogen atoms are omitted)

There are two crystallographically independent Cu atoms (Cu1 and Cu2) in the asymmetric unit for compound **1**. This way, Cu1...Cu2 and Cu2...Cu1<sup>i</sup> (*i*= x, 1+y, z) distances for compound **1** are 7.2483(4) Å and 7.2436(4) Å, respectively. Cu1-Cu2-Cu1<sup>i</sup> angle is 75.640°(4). In the case of compound **2**, the Cu1...Cu1<sup>i</sup> (*i*= 1/2-x, -1/2+y, 1/2-z) distance is 8.0719(5) Å, and Cu1<sup>ii</sup>-Cu1-Cu1<sup>i</sup> (*x*, 1/2-y, z) angle is 74.854°(4).

In both cases, Cu-O distances lie within the range 1.934(2)-2.259(2) Å, and Cu-N distances exhibit values between 1.992(2) Å and 2.0366(2) Å (tables 2 and 3).



In summary, the same synthon (Cu–PDC–0.5bpa–H<sub>2</sub>O) produces herringbone arrays with quite different features. In fact, as observed in figure 5, the 2D array for **2** is closer to an ideal 3-c herringbone (where metal atoms should be coplanar). Thus, these differences influence on the stacking mode.

As observed in figure 8, packing of these layers takes place along the [101] direction for both compounds. The packing is, obviously, influenced by the crystallization molecules. The layers in **1** are packed according to an A-A-A fashion. However, the packing for **2** follows an A-B-A fashion due to a displacement of the layers.

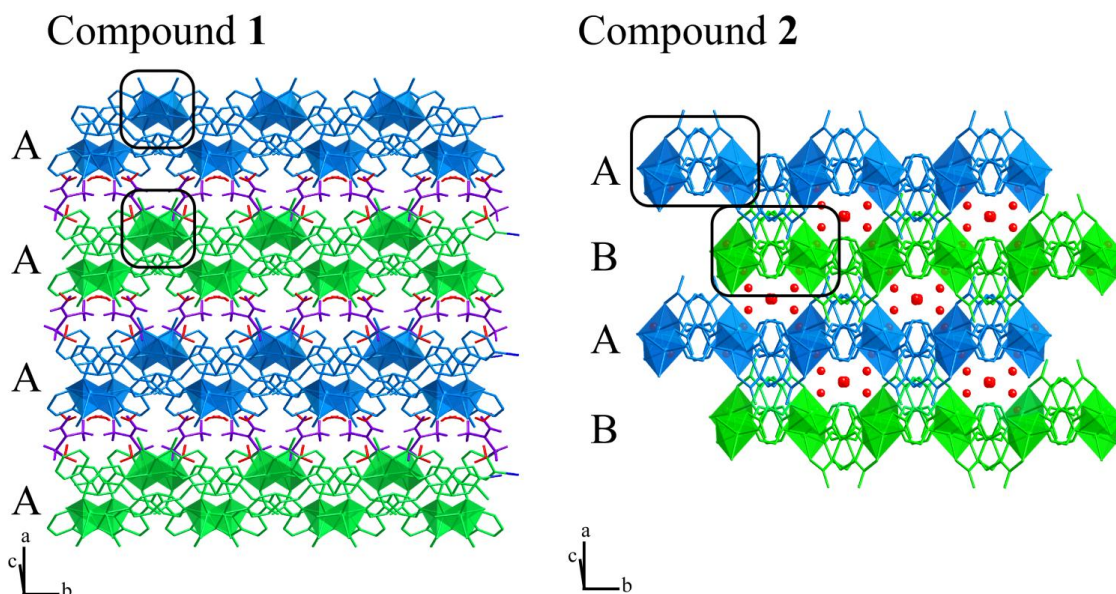
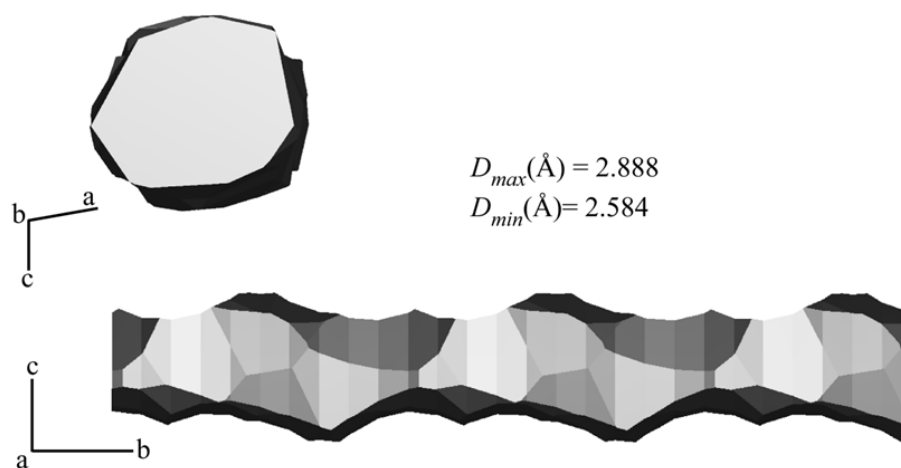


**Figure 8** Packing for (left) compound **1** and (right) compound **2**, showing the A-A-A and A-B-A disposition of the layers, respectively. Crystallization molecules of water are shown in red, and DMF molecules in violet (all hydrogen atoms are omitted for clarity).

The disposition of the herringbone-type layers in compounds **1** and **2** gives rise to channels along the [010] direction. The diameter of the channels has been evaluated by means of the Voronoi-Dirichlet polyhedra, which were constructed through the Dirichlet program included in TOPOS [5] (figure 9). The dimensions of these channels are 2.888 Å x 2.584 Å for **1**, and 3.150 Å x 2.014 Å for **2**. On the other hand, the interlayer distances are quite different for both compounds. Minimum and maximum intermetal distances are 7.858 Å and 11.479 Å for **1**, and 6.366 Å and 7.155 Å for **2** (figure 10). The fact that compound **2** is nearer the ideal 3-c herringbone array permits the planes to be closer.

### Compound 1



### Compound 2

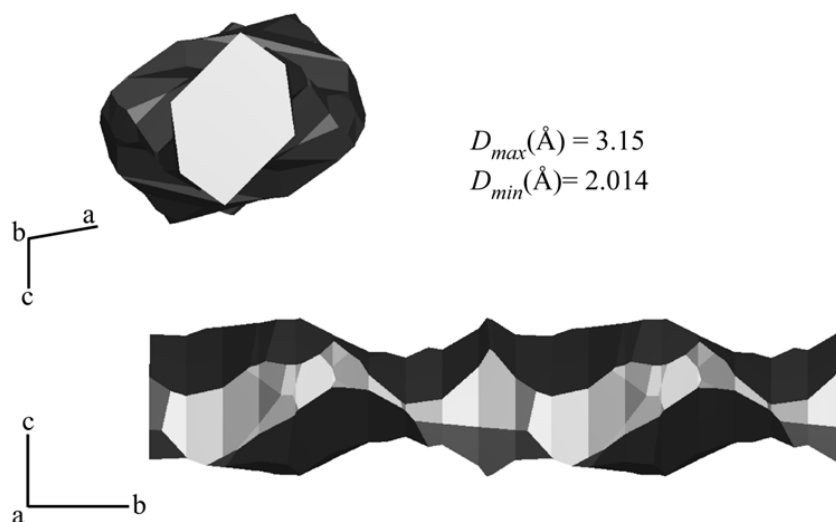
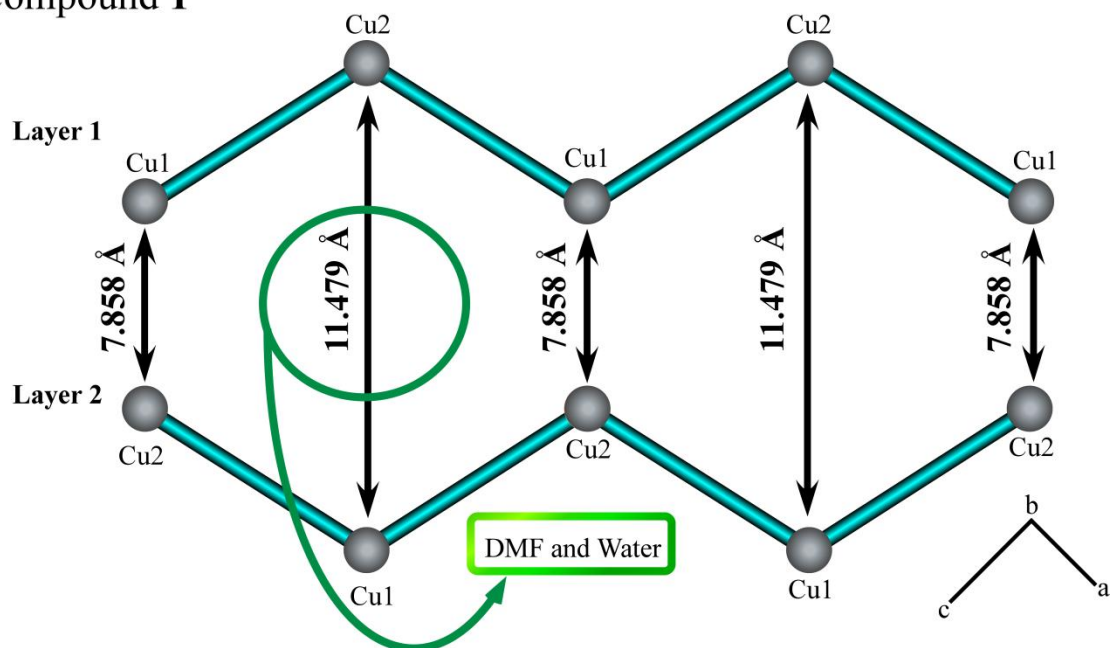


**Figure 9.** Voronoi-Dirichlet representations for the channels observed for compounds **1** and **2**.

### Compound 1



### Compound 2

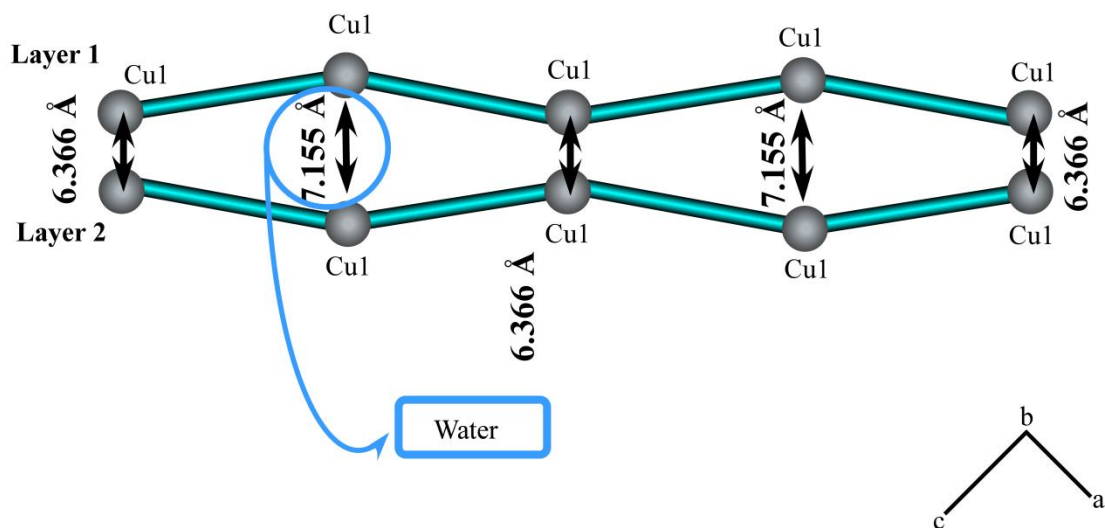


**Figure 10.** Interlayer distances for compounds **1** and **2**.

Topological features for compounds **1** and **2** were analyzed by means of the TOPOS [5] software, revealing a hcb Shubnikov hexagonal plane net (Point symbol =  $6^3$  and vertex symbol = [6.6.6]), corresponding to the topology shown in figure 11.

Herringbone 3-connected topology

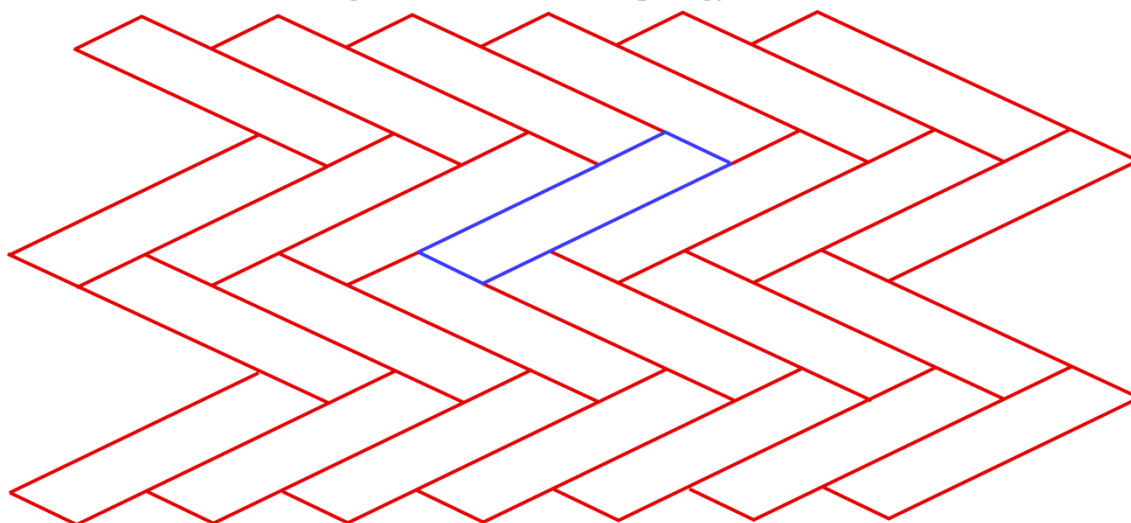


**Figure 11.** 2D herringbone array based on three-connected nodes.

The distortion of coordination polyhedra was evaluated according to Avnir method [6,7] based on the continuous symmetry measures (CSM), by means of SHAPE program [8], and the results can be seen on table 6. The projection of the as-calculated values on the distortion diagram can be seen in figure 12. As observed for the three analyzed Cu<sup>II</sup> ions, distortion is on a non-Berry pathway that converts the trigonal bipyramid into a square pyramid [9] (SPY) with a soft contribution of a vacant octahedron (VOC) distortion. In fact, for Cu1 and Cu2 in compound **1**, the axial distances (Cu1-O2W=2.2488(2) Å and Cu2-O1W=2.2197(2) Å) are longer than the equatorial ones (going from 1.9340(2) Å to 2.0366(2) Å). Similarly, for compound **2**, the axial distance Cu1-O5W is 2.259(2) Å, and the equatorial ones go from 1.9737(2) Å to 1.999(2) Å.

**Table 6** Geometrical distortions of the trigonal bipyramid (TBPY) and Berry square pyramid (SPY), calculated using SHAPE software.

Compounds	Pentacoordinate	S(TBPY)	S(SPY)
Compound <b>1</b>	Cu(1)	5.73	1.20
	Cu(2)	5.47	1.08
Compound <b>2</b>	Cu(1)	4.40	0.75

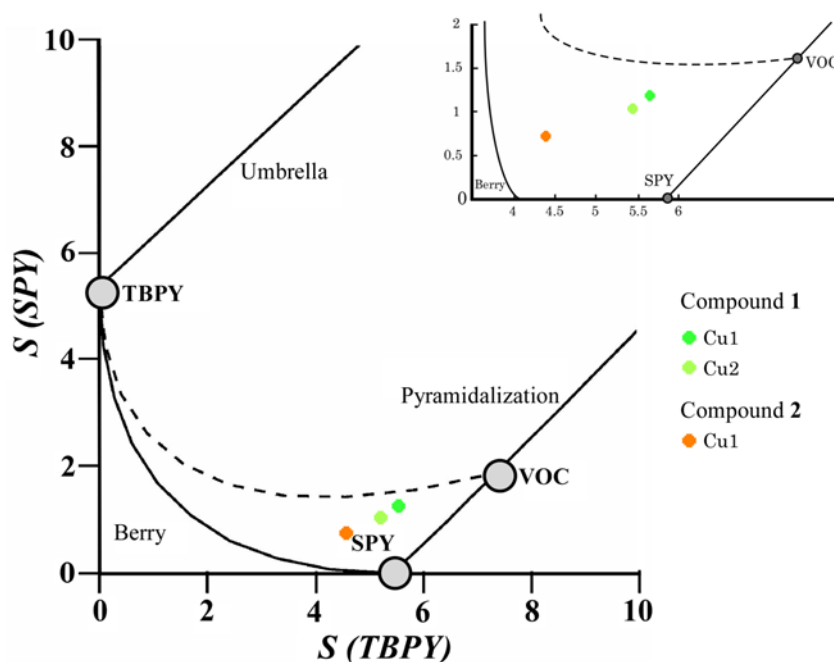
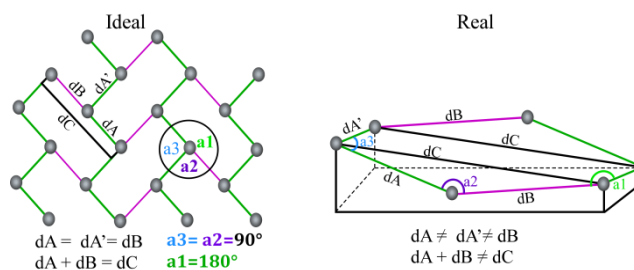


**Figure 12.** Distortion modes diagram of a pyramidal based squared coordination environment. In the upper right is a zoom of the distortion for compound **1** Cu1 (green) and Cu2 (green light), and for compound **2** Cu1 (orange).

## 2.2. Herringbone mapping

As said before, we elsewhere reported a mapping of the herringbone-type structures identifying two types of arrays depending on the number of connections for each metal ion: this is, 4-connected (4-c) or 3-connected (3-c). Furthermore, we identified the structural parameters defining the 3-c herringbone arrays, correlating angles and distances (Scheme 2) [4,10-18].

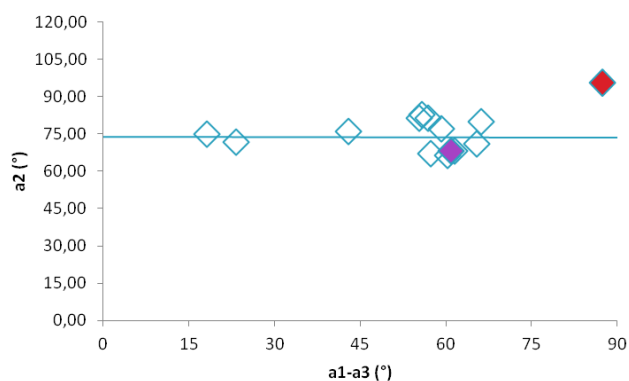


**Scheme 2.** (Left) Ideal high symmetry plane for a 3-c herringbone array, and (right) real non-coplanar herringbone array.

Representative values for compounds **1** and **2** are shown in table 7. Representation of these values can be seen in figure 13. As observed, compound **1** lies on the typical zone around  $a1$ - $a3 \approx 60^\circ$  and  $a2 \approx 75^\circ$ . On the other hand, as far as we are concerned, values for **2** indicate that this compound is the closest one to an ideal 3-c herringbone reported so far (ideality referred to angles). Obviously, the fact that  $a1+a2+a3$  for **2** is  $332.50^\circ$  (this is, close to  $360^\circ$  which is the value corresponding to coplanarity) is in accordance with the later. For compound **1**,  $a1+a2+a3 = 280.15^\circ$ . This is a habitual value for similar arrays.

**Table 7** Structural parameters for compounds **1** and **2**.

	<i>Compound 1</i>	<i>Compound 2</i>
<b>a1</b> (°)	136.48	162.19
<b>a2</b> (°)	68.03	95.46
<b>a3</b> (°)	75.64	74.85
<b>dA</b> (Å)	7.25	8.07
<b>dB</b> (Å)	13.45	13.33
<b>dB*</b> (Å)	12.11	13.09
<b>a1-a3</b>	60.84	87.34

**Figure 13** Representation of the  $a_2$  parameter vs. the  $a_1$ - $a_3$  parameter for the herringbone arrays found in literature. Compounds **1** (purple) and **2** (red) are marked by filled symbols.

### 2.3. Thermogravimetry

In order to study the thermal stability of compounds **1** and **2**, thermogravimetric (TG) analysis was performed.

Compound **1** shows two-stages of mass loss (figure 14). The first of them, starting at RT and finishing at about 245 °C, has been assigned to the removal of the crystallization and coordination molecules of water and DMF (20.1% calc. and 18.32% exp.). The second one (63.35% calc. and 61.38% exp.) is an abrupt mass loss, and corresponds to the removal of both organic ligands occurring between 245 °C and 340 °C. The residue has been identified by X-ray powder diffraction as CuO.<sup>55</sup>

The TG analysis of compound **2** shows a weight loss of 17.1% from RT to 100°C (figure 15), attributed to the crystallization and coordination molecules of water (18.5% calc). The curve shows a plateau up to 225°C, when the calcination of the organic molecules takes place with a weight loss of 60.1% (63.1% calc.). The calcination product was also CuO [55].

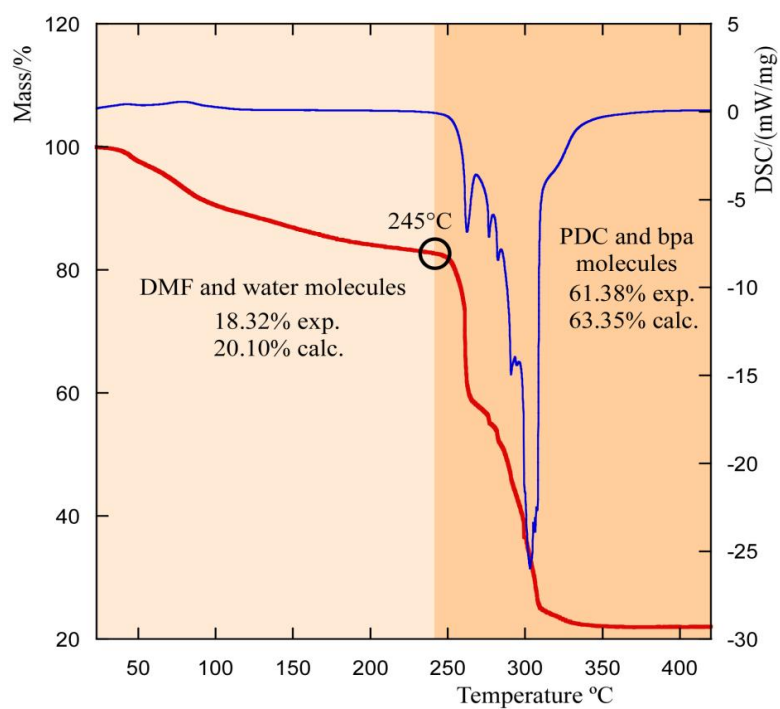


**Figure 14.** Thermogravimetric analysis for compound **1**. Orange ranges show the weight loss intervals.

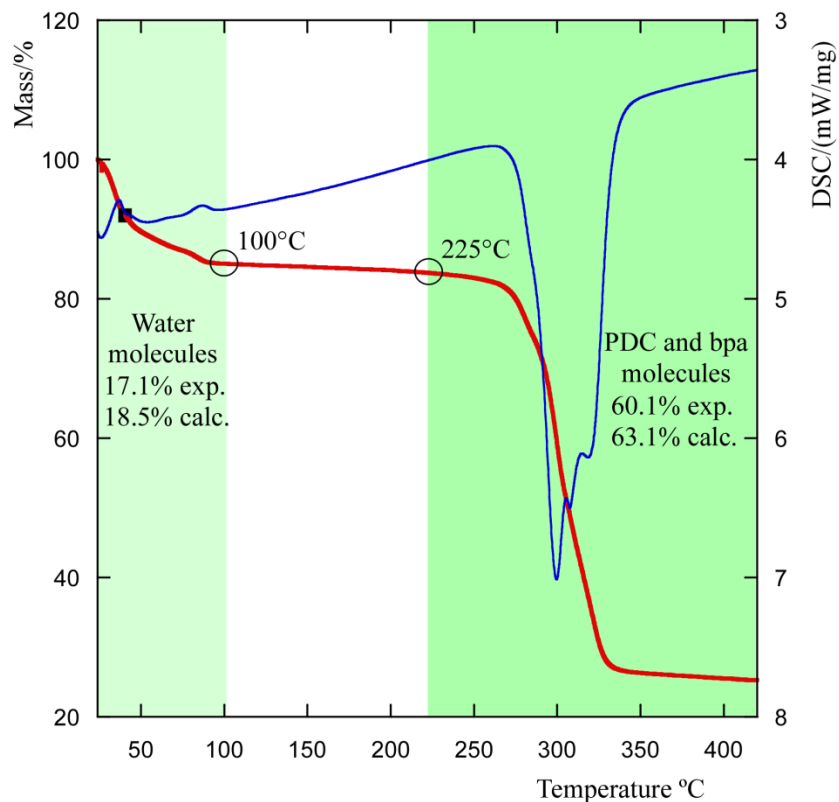


**Figure 15.** Thermogravimetric analysis for compound **2**. Green ranges show the weight loss intervals.

## Acknowledgements

This work has been financially supported by the “Ministerio de Economía y Competitividad” (MAT2013-42092-R, FEDER MAT2010-21342-C02-01), the “Gobierno Vasco” (Basque University System Research Group, IT-630-13) and UPV/EHU (UFI 11/15) which we gratefully acknowledge. SGIker (UPV/EHU) technical support is gratefully acknowledged. F. Llano-Tomé thanks the “Ministerio de Ciencia e Innovación” for a fellowship (BES-2011-045781).

## References

1. Yinghua W (1987) Lorentz-polarization factor for correction of diffraction-line profiles. *J Appl Crystallogr* 20:258-259.
2. Altomare A, Cascarano G, Giacovazzo C, Guagliardi A (1993) Completion and refinement of crystal structures with SIR92. *J Appl Crystallogr* 26:343-350.
3. Sheldrick GM (2008) A short history of SHELX. *Acta Crystallogr Sect A* 64:112-122.
4. Llano-Tomé F, Bazan B, Urriaga MK, Barandika G, Lezama L, Arriortua MI (2014) CuII–PDC–bpe frameworks (PDC = 2,5-pyridinedicarboxylate, bpe=1,2-di(4-pyridyl)ethylene): mapping of herringbone-type structures. *CrystEngComm* 16:8726-8735.
5. Blatov VA (2014) ToposPro: The program package for multipurpose geometrical and topological analysis of crystal structures. <http://topospro.com>. Accessed 21 March 2015.
6. Zabrodsky H, Peleg S, Avnir D (1992) Continuous symmetry measures. *J Am Chem Soc* 114:7843-7851.
7. Pinsky M, Avnir D (1998) Continuous Symmetry Measures. 5. The Classical Polyhedra. *Inorg Chem* 37:5575-5582.
8. Llunell DCM, Cirera J, Bofill JM, Alemany P, Álvarez S, Pinsky M, Yanutir D (2003) SHAPE v1.1a.
9. Alvarez S, Alemany P, Casanova D, Cirera J, Llunell M, Avnir D (2005) Shape Maps and Polyhedral Interconversion Paths in Transition Metal Chemistry. *Coord Chem Rev* 249:1693-1708.
10. Lin J, Wen L, Zang S, Su Y, Lu Z, Zhu H, Meng Q (2007) A novel 2D herringbone-like zinc coordination polymer built from helical motif: Hydrothermal synthesis, structure and properties. *Inorg Chem Commun* 10:74-76.
11. Rogers CM, Murray NH, Supkowski RM, La Duca RL (2013) Cadmium carboxycinnamate coordination polymers with dimensionality differences depending on dipyrindyl ligand. *Inorg. Chim Acta* 407:167-174.
12. Shyu E, Braverman MA, Supkowski RM, LaDuca RL (2009) Control of topology and dimensionality by aromatic dicarboxylate pendant arm position and length in cadmium coordination polymers incorporating a hydrogen-bonding capable kinked dipyrindine ligand. *Inorg Chim Acta* 362:2283-2292.
13. Sengupta S, Ganguly S, Goswami A, Sukul PK, Mondal R (2013) Identification of a robust and reproducible noncluster-type SBU: effect of coexistent groups on network topologies, helicity, and properties. *CrystEngComm* 15:8353-8365.
14. Wen DC, Liu SX, Ribas J (2007) Syntheses, structures and magnetic property of two copper complexes with cyclic dimer and 2D herringbone-like network built from helical motif. *Inorg. Chem Commun* 10:661-665.
15. Withersby MA, Blake AJ, Champness NR, Cooke PA, Hubberstey P, Schroder M (1999) Parallel interpenetration in novel herringbone sheets formed by Co(II) and Cd(II) complexes with trans-4,4'-azobis(pyridine). *New J Chem* 23:573-575.
16. Meng WL, Zhang ZH, Lv Y, Kawaguchi H, Sun WY (2006) Synthesis, crystal structure and magnetic property of a two-dimensional herringbone-like network with praseodymium(III) nitrate and 1-bromo-3,5-bis(imidazol-1-ylmethyl)benzene (bib). *Appl Organomet Chem* 20:399-403.



17. Kondo M, Shimamura M, Noro SI, Minakoshi S, Asami A, Seki K, Kitagawa S (2000), Microporous Materials Constructed from the Interpenetrated Coordination Networks. Structures and Methane Adsorption Properties. *Chem Mater* 12:1288-1299.
18. Withersby MA, Blake AJ, Champness NR, Cooke PA, Hubberstey P, Realf AL, Teat SJ, Schroder M (2000) Engineering of co-ordination polymers of trans-4,4'-azobis(pyridine) and trans-1,2-bis(pyridin-4-yl)ethene: a range of interpenetrated network motifs. *Dalton* 3261-3268.